Argonne NATIONAL LABORATORY

ANL-22/74

Updated Production Inventory for Lithium-Ion Battery Anodes for the GREET® Model, and Review of Advanced Battery Chemistries

Energy Systems and Infrastructure Analysis Division

ANL-22/74

Updated Production Inventory for Lithium-Ion Battery Anodes for the GREET® Model, and Review of Advanced Battery Chemistries

by
Rakesh Krishnamoorthy Iyer and Jarod C. Kelly
Energy Systems and Infrastructure Analysis Division, Argonne National Laboratory

October 2022

CONTENTS

FIGURES

TABLES

ACKNOWLEDGMENTS

This activity was supported by the Vehicle Technologies Office, Office of Energy Efficiency and Renewable Energy, United States Department of Energy under Contract Number DE-AC02-06CH11357. The authors would like to thank Steven Boyd and Samm Gillard of that Office for their guidance and support. The views and opinions of the authors expressed herein do not necessarily state or reflect those of the U.S. Government or any agency thereof. Neither the U.S. Government nor any agency thereof, nor any of their employees, makes any warranty, expressed or implied, or assumes any legal liability or responsibility for the accuracy, completeness, or usefulness of any information, apparatus, product, or process disclosed, or represents that its use would not infringe privately owned rights.

ACRONYMS

APAC	Asia & Pacific
BatPaC	Battery Performance and Cost
CH_4	Methane
CO	Carbon Monoxide
Co	Cobalt
CO_2	Carbon Dioxide
EV	Electric Vehicle
GREET®	Greenhouse gases, Regulated Emissions and Energy use in Transportation
HSP	High Softening Point
KCl	Potassium Chloride
LCA	Life-Cycle Analysis
LCI	Life-Cycle Inventory
Li	Lithium
Li_2CO_3	Lithium Carbonate
Li-A	Lithium-Air
LIB	Lithium-Ion Batteries
LiCl	Lithium Chloride
$LiOH.H_2O$	Lithium Hydroxide
Li-S	Lithium-Sulfur
LTO	Lithium Titanate
LWG	Length-Wise Graphitization
NG	Natural Graphite
NO_x	Nitric Oxide
NT	Nanotubes
NW	Nanowires
SG	Synthetic Graphite
Si	Silicon
SSB	Solid-State Battery
TEOS	Tetraethyl Orthosilicate
USGS	United States Geological Survey

ABSTRACT

The Greenhouse gases, Regulated Emissions, and Energy use in Technologies (GREET®) model considers lithium-ion batteries with multiple anode materials. Synthetic graphite is the primary anode material used in the previous GREET versions, even as the model offered options to choose a lithium anode and/or a blended anode (blend of synthetic graphite and silicon). Yet, the inventory (material and energy flows) considered for these anodes is dated, and the anode options do not consider natural graphite, which is another important anode material for lithium-ion batteries. This report documents the material and energy flows for natural graphite anode production from raw material extraction to anode production – as incorporated in the updated GREET model. We also present a brief literature review on the current state of inventory for the other three anodes (synthetic graphite, silicon, and lithium), as well as updates made in the recent GREET model on material and energy flows associated with their respective production. Finally, this study provides a summary of advanced battery systems that may be alternatives to LIBs for use in future electric vehicles.

1 INTRODUCTION

The global drive to reduce greenhouse gas and local pollutant emissions has led to a drastic rise in the demand for electric vehicles (EVs) across both passenger and freight transportation (Stringfellow and Dobson, 2021; Toba et al., 2021). This has increased the demand for lithium-ion batteries (LIBs) due to several advantageous properties, such as their long cycle life, high specific capacity, low maintenance requirements, and wide window of operational temperature (Agubra and Fergus, 2013; Yang et al., 2021; Zuo et al., 2017). LIBs are composed of multiple important constituents (Dunn et al., 2015, 2014), including the cathode and anode, which are both extremely important to EV battery performance (Agubra and Fergus, 2013). Also, a sustained and robust supply of battery anode materials (much like other battery-related materials) is vital to meeting both the demand for LIBs for transportation and the United States' climate change goals (CoP26, 2021; Olivetti et al., 2017; US DoE, 2011).

Commercially, graphite is the most commonly used anode in LIBs – used in both natural as well as synthetic forms – because of its superior capacity retention over long-term cycling (Yang et al., 2021). However, graphite is also plagued by low theoretical gravimetric capacity (372 mAh/g) and major safety concerns like lithium plating and dendrite formation (Agubra and Fergus, 2013; Yang et al., 2021; Zhang et al., 2021; Zuo et al., 2017). Moreover, while the United States remains a major producer of synthetic graphite (SG), it is entirely dependent on imports for natural graphite (NG) (USGS, 2022). Ongoing efforts to address the issues with graphite focus on developing alternative anodes, with lithium (Li) and silicon (Si) anodes being the two prominent anodes of interest due to their superior properties (Ding et al., 2019; Wang et al., 2020; Zuo et al., 2017). However, these efforts also face their own challenges, such as lithium's status as a US critical material (US DoE, 2011; US DOE, 2020).

The criticality of LIB anode materials for the US makes it imperative to assess their consequences from different perspectives. A key aspect of this assessment is to understand the environmental benefits and challenges of different anode materials, especially given the advantages cited in favor of shifting from petroleum-based vehicles to EVs (Dunn et al., 2014; Wu et al., 2018). Typically, such benefits are demonstrated using life-cycle analysis (LCA) – a methodology commonly used to evaluate the environmental impacts of products and services across their entire life-cycle (Hellweg et al., 2014). Numerous LCA studies have been conducted to determine and compare the environmental impacts of EVs with petroleum-based vehicles (Dolganova et al., 2020; Verma et al., 2022), including using Argonne's GREET® model (Asaithambi et al., 2019; Dai et al., 2019; Kelly et al., 2022; Lai et al., 2022; Shafique and Luo, 2022; Yin et al., 2021). Overall, the studies highlight the significance of LIBs for an EV's environmental performance, particularly during its vehicle-cycle (i.e., production phase), and attribute it to several factors, with anodes playing a notable role (Dai et al., 2019; Kelly et al., 2019; Winjobi et al., 2022). However, the material and energy flows for anodes in studies based on the previous GREET versions are based on an earlier report (Dunn et al., 2015) and would benefit from an update. In light of recent technological advancements, these flows need to be revised to conduct an up-to-date environmental analysis of LIBs, and thereby, EVs. Moreover, the previous GREET versions provide material and energy flows for three anode materials (synthetic graphite, silicon, and lithium) but do not provide similar data for natural graphite. This

needs to be addressed, both due to the significant cost advantages of natural graphite over its synthetic counterpart (Bennett, 2021; Bhatuda, 2021; Northern Graphite, 2021) and also due to its criticality as a resource for the US to fulfill its LIB needs for EVs (US DoE, 2011; US DOE, 2020).

This report provides a detailed literature review on the life-cycle inventory (LCI, or material and energy flows) for all four LIB anodes – natural and synthetic graphite, lithium, and silicon – updating the last report published by Argonne National Laboratory on this subject (Dunn et al., 2015) (Section 2). It also details the LCI for industrial production of these anodes, where such data are available (Section 2). In the final section (Section 3), we shift from LIBs to other alternative battery systems that could play a major role in future EVs, primarily due to their specific advantages over LIBs. These systems are currently not included in the updated GREET model, but they represent potential future pathways in the EV market and are thus important to understand and track.

2 LIB ANODES: LITERATURE REVIEW & LIFE-CYCLE INVENTORY (LCI)

Four different LIB anodes are considered in this study: natural graphite (NG), synthetic graphite (SG), silicon (Si), and lithium (Li). Details on their relevance for LIBs, availability in the United States, and their respective material and energy flows are provided in the subsections below.

2.1 Graphite (Natural & Synthetic)

2.1.1 Significance & Availability

Graphite has been the default anode since the 1980s (Zhang et al., 2021), and its current market dominance (89% share of all LIBs) is expected to continue in the future (Engels et al., 2022; Pillot, 2019). This is due to its several beneficial features, including its long cycle life, high thermal and electrical conductivity, high energy density and temperature resistance, and lower cost compared to other anode options (Graphite Corp., 2021; Zhang et al., 2021). Graphite is used in LIBs in substantial amounts (15-20 wt.% of battery) (Dai et al., 2019; Dolganova et al., 2020; Shafique and Luo, 2022; M. Wang et al., 2021). Its market dominance and substantial use per battery make graphite's availability paramount for any further rise in the market share of EVs.

Two forms of graphite are used as LIB anodes: NG (or more specifically, flake graphite), and SG, roughly in a 50:50 ratio (Hao et al., 2016; Qatar Green Leaders, 2019). While NG is extracted from natural minerals in the ground, SG is produced via high-temperature processing of carbon precursors such as petroleum coke and coal tar pitch (Vohler et al., 2021). Both forms of graphite anodes are polycrystalline, consisting of multiple single-crystal domains (Asenbauer et al., 2020; Jara et al., 2019; Rui et al., 2022). They also offer their respective properties, which are listed in Table 1. NG is less costly than SG since SG production incurs higher energy costs through energy-intensive processing of unsaturated carbon resources (like petroleum coke) for long durations (Asenbauer et al., 2020; Jara et al., 2019; Vohler et al., 2021). NG anodes are also known to offer larger gravimetric capacity than SG due to the larger size of their crystalline domains (Asenbauer et al., 2020). On the other hand, SG offers advantages over NG, such as its high purity and thermal stability, low thermal expansion, and the ability to produce SG from relatively abundant resources compared to the classification of NG as a critical material at least in the US (Asenbauer et al., 2020; Jara et al., 2019; US DoE, 2011; US DOE, 2020). Further, SG is known for its better quality (in terms of its superior lithiation/de-lithiation kinetics), reproducibility (its consistency in properties across different batches of production), and operational life vis-à-vis NG (Asenbauer et al., 2020; Jara et al., 2019).

Table 1: Natural Graphite (NG) v/s Synthetic Graphite (SG) – A Comparison (Asenbauer et al., 2020; Bennett, 2021; Jara et al., 2019; Rui et al., 2022)

Properties/Parameters	Natural Graphite (NG)	Synthetic Graphite (SG)
Source of production	Ores within ground	Carbon precursors (e.g., petroleum coke, coal tar pitch)
Production cost	Relatively low	Relatively high
Purity	Low	High
Quality	Low	High (better thermal stability, lower thermal expansion)
Performance in LIBs	Relatively low (anisotropic orientation of crystals)	Relatively high (isotropic orientation of crystals ensures superior lithiation/de-lithiation kinetics)
Capacities	High (due to higher domain size)	Low (due to smaller domain size or more inter-domain interfaces)
Cycle life	Short	Long

In terms of their production sources, China is the largest global producer of both forms of graphite, accounting for over 70% of their respective production (Northern Graphite, 2021; USGS, 2022). The US did not produce any NG in 2021, importing all of its needs from China (33%), Mexico (21%), Canada (17%), India (9%), and other nations (collectively 20%) from 2017 to 2020 (USGS, 2022). North America (U.S., Canada, and Mexico) accounted for ~12% of global NG production in 2021 (USGS, 2022). For NG, in our literature review, we did not obtain any references with sufficient clarity on either the total global SG production or the share of the United States in this global production. Nevertheless, as per the US Geological Survey (USGS) (USGS, 2022), the country produced 276,000 metric tons of SG in 2019 – roughly 85% of its total domestic consumption in that year. SG is used for a variety of applications, including in foundries, LIB anodes, bipolar plates in fuel-cells, coatings, friction materials, electrolytic processes (such as for steel), corrosion products, and as fillers in plastic and rubber products (Surovtseva et al., 2022). However, data on the exact amount of SG use as battery anodes was not available in the literature.

2.1.2 Synthetic Graphite Manufacturing

Previous versions of the GREET model have considered the production of SG from petroleum coke and coal tar pitch, and a complete description of this manufacturing process is provided in an earlier report by Argonne National Laboratory (Dunn et al., 2015). Figure 1 shows the schematic for SG production, which is typically done through three distinct processes that are conducted separately (Surovtseva et al., 2022). First, green petroleum coke is produced either via petroleum refining or by cracking heavy oils in the presence of a catalyst. Next, green coke is calcined to produce needle coke, which is then ground to the desired size, impregnated with a binder (coal tar pitch), and then baked at 850-1300°C to condition it. The conditioned needle coke is graphitized at > 2500°C to produce high-quality, high-purity SG (Surovtseva et al., 2022; Vohler et al., 2021). The last step is post-processing, which can include any of milling,

shaping, classification, or coating processes to ensure safe packaging of SG. However, there is a lack of information in the literature on whether these post-processes are needed separately after SG production, as many of them have already been used in the processes *en route* to its production (Surovtseva et al., 2022). Hence, we have not included these processes in the schematic or in considering material and energy flows for SG production in the updated GREET model.

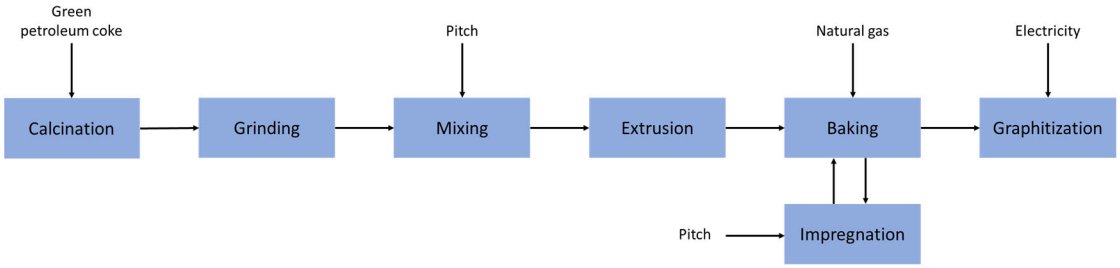

Figure 1: Schematic for Commercial Production of Synthetic Graphite (SG) (reproduced from (Dunn et al., 2015))

2.1.3 Material and Energy Flows for Synthetic Graphite Production

Since Argonne's previous publication on LCI (material and energy flows) for SG production (Dunn et al., 2015), only a few studies have provided more-recent LCI data on this topic. Rui et al. (2022) have computed the cradle-to-gate emergy[1] input of NG and SG anodes, as an indicator of their respective environmental impacts. They provide the commercial-scale material and energy flow inputs for producing both types of anodes, and report lower emergy input for SG anodes, indicating it as an environmentally preferable option to NG anodes (Rui et al., 2022). However, a more detailed LCI is reported by Surovtseva et al. (2022), who have provided detailed material and energy flows and emission outputs for all stages beginning with the production of concerned fossil fuels (coal/petroleum products) to the final production of SG as output. Hence, we have used the LCI from this study to inform our update of the material and energy flows for SG production in the updated GREET model, while making specific modifications based on other references as necessary.

The first four stages in the reported LCI of SG production in Surovtseva et al. (2022) deal with coal production, production of coal tar pitch from coal, crude oil mining and transmission, and crude oil refining. Since these stages are already covered in the GREET model, we have not included them separately in the material and energy flow entries for SG production, and instead, used their data directly from GREET. It is the remaining three steps – calcination of green coke to needle coke, baking, and graphitization – that we have incorporated into the updated GREET model from (Surovtseva et al., 2022).

[1] Emergy refers to the total sum of all solar energy that is needed to produce a product or service (ref).

For calcination, Surovtseva et al. (2022) assumes a material yield of 74%, meaning that 0.74 kg of needle coke is produced from 1 kg of green petroleum coke, with the remaining material lost as atmospheric emissions (CO_2, CO, and CH_4). Subsequently, for baking, needle coke and coal tar pitch are used in a ratio of 80:20 (needle coke: coal tar pitch) by weight to produce the precursor for graphitization, assuming a mass loss of 0.4% in this process (Bogacki et al., 2012). Thus, 0.8 kg of needle coke and 0.2 kg of coal tar pitch react in the baking setup to produce 0.996 kg of graphitization precursor, with the remaining material emitted as gases (Surovtseva et al., 2022).

The final step – graphitization – is conducted exclusively in one of two electric furnaces: Acheson, or Castner (also known as length-wise graphitization or LWG furnace) (Daimer, 2021). Argonne's previous report on LCI of SG assumes its production using an Acheson furnace (Dunn et al., 2015). However, Castner (LWG) furnaces have been increasingly replacing their Acheson counterparts over the past few years due to their higher energy efficiency, lower cost due to smaller furnace sizes, and improved homogeneity in their final product (Daimer, 2021). Hence, we assume the Castner furnace for the graphitization process in the updated GREET model. Since Daimer (2021) provides more recent data on energy (electricity) consumption for graphitization in LWG furnaces, we have used their data for energy consumption of this process in the updated GREET model (2-3 kWh/kg of graphite). However, for the assumed mass loss in this process (2%) and the resultant emissions from graphitization – taken from Bogacki et al (2010) – we consider the LCI values reported in (Surovtseva et al., 2022).

Table 2 provides the material and energy flows for SG production across the calcination, baking, and graphitization steps. Two other assumptions have been made regarding energy use and emission calculations for SG production. First, due to the lack of background inventory on coal tar pitch in our literature review, we consider its LCI to be the same as that for coke produced from coal in the updated GREET model. Second, unlike the previous GREET model versions that assumed SG to be produced in China, we only consider SG production in the United States. This is because the USGS data (USGS, 2022) indicates that the vast majority (~85%) of the country's SG demand is met by domestic production. All the material and energy flows are provided in the Anode sheet of GREET2 in the updated GREET model.

Table 2: Material and Energy Flows for Synthetic Graphite (SG) Production (Surovtseva et al., 2022)

Inputs	Calcination	Carbonization/ Baking	Graphitization
Material inputs (ton/ton of SG)			
Green petroleum coke	1.108		
Coal tar pitch		0.205	
Energy inputs (mmBtu/ton of SG)			
Natural gas	13.566	11.091	
Electricity	1.507		7.711
Process emissions (g/ton of SG)			
CO	14,067	2,482	17,866
NO_X		229	
CH_4	155,740	73.9	
CO_2	13,062		

2.1.4 Natural Graphite Manufacturing

Figure 2 shows the schematic for cradle-to-gate production of NG as per Engels et al (2022) in China, which is its biggest global producer (Northern Graphite, 2021; USGS, 2022). This schematic and its description are provided in Engels et al (2022), and a summary of the same is provided below.

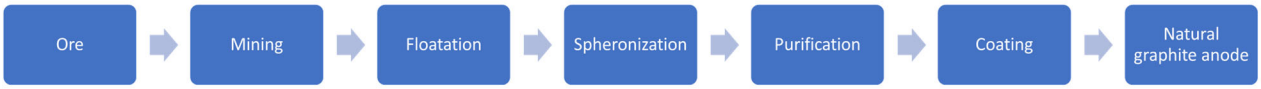

Figure 2: Schematic of Natural Graphite Production, based on (Engels et al., 2022)

Graphite ore (carbon content: 11%) is mined primarily via open cast mining (includes drilling and blasting), and transported to a floatation facility. Here, the ore is first crushed and milled, and then subjected to a multi-step flotation process to achieve a concentrate with high carbon content (85-98%). Flotation is used due to graphite's hydrophobic nature, which makes it easier to remove it from the agent. It is conducted using grinding mills, water and pine oil as flotation agents, and diesel as a collector. The wet carbon concentrate obtained from flotation is dried and heated using coal, and only small flakes are used for further processing. In the next step (spheronization), these flakes pass through multiple classifier mills (arranged in a row) to get spherical graphite particles with three desired properties: narrow particle size distribution, high tap density, and low specific surface area. A key byproduct of this step is graphite fines, that constitute 60% of total output from this process. These fines are used in pencils, refractories, carbon raisers, and as precursor for further flake size reduction. Usable spherical graphite (from spheronization) is then sent for purification to remove impurities (such as aluminum, calcium, chlorine, chromium, nickel, sulfur, silicon, and zinc) and increase its carbon content (to > 99.95%). Purification is done by chemically leaching spherical graphite with acids (hydrofluoric,

hydrochloric, and nitric), and then treating with an alkaline reagent (quicklime) to neutralize the left-over acids before disposal.

The last major step is coating, where purified graphite particles are modified to enhance both their conductivity and hardness, and to seal their surfaces to ensure that fewer Li ions are lost during the initial charging cycles in LIBs. Coating itself is a three-stage process. First, purified spherical graphite particles are mixed with the coating material (high softening point pitch or HSP pitch). Next, the mixture is put in a furnace and melted to form a uniform coating layer on these particles. In the final stage, the coating is carbonized by heating the coated particles in a furnace for 15-16 hours in an inert atmosphere. An after-treatment finishing step is also used to de-agglomerate the particles that merged in the carbonization furnace, sieve them, remove magnetic impurities, and homogenize the product particles before packing them.

2.1.5 Material & Energy Flows for Natural Graphite (NG) Production

As mentioned earlier, Rui et al. (2022) analyzed the cradle-to-gate emergy[2] input of NG and SG anodes, and reported commercial-scale material and energy flows for their respective production. Apart from this study, we obtained three studies with LCI data for NG production from literature, all of which focus on NG production in China – the biggest global NG producer (USGS, 2022). Two of these three papers provide the combined LCI for NG production encompassing all the major steps listed in Figure 2 (Gao et al., 2018; Zhang et al., 2018). In contrast, Engels et al. (2022) provide the most detailed, stage-by-stage material and energy flows for NG production from China. Since China is the biggest source of NG imports for the US and its biggest global producer (USGS, 2022), we have incorporated this stage-by-stage LCI from Engels et al. (2022) in the updated GREET model. These flows are provided in Table 3.
.

[2] Emergy refers to the total sum of all solar energy that is needed to produce a product or service (ref).

Table 3: Material & Energy Flows for Natural Graphite (NG) Production (Engels et al., 2022)

Inputs/Outputs	Mining	Flotation	Spheronization	Purification	Coating
Material outputs (ton of intermediate output product in each stage)					
Graphite ore	1				
Graphite concentrate		1			
Spherical graphite			1		
Spherical purified graphite				1	
Coated spherical graphite					1
Graphite fines			1.215		
Material inputs used (ton/ton of intermediate product)					
Graphite ore		9.59			
Graphite concentrate			2.22		
Spherical graphite				1.13	
Spherical purified graphite					1.01
Ammonium nitrate	2.48×10^{-4}				
Pine oil		1.16×10^{-3}			
Diesel	1.20×10^{-5}	1.55×10^{-3}			
Ceramic grinding media		0.009			
Hydrofluoric acid				0.18	
Hydrochloric acid				0.20	
Nitric acid				0.10	
Water		0.022		0.025	
Lime				0.40	
HSP oil					0.05
Nitrogen					0.0015
Energy Inputs (mmBtu/ton of intermediate product)					
Electricity	0.027	1.561	6.478	0.941	14.034
Diesel	0.082	0.037	0.015	0.009	0.009
Coal		1.132			
Natural gas				0.905	
Emissions (g/ton of intermediate product)					
NO_x	125.19				
CO_2	36.29	166,317		52,390	56,615

2.2 Silicon Anodes

2.2.1 Availability & Significance

Silicon (Si) is the second-most abundant material inside the earth's crust after oxygen, accounting for ~28% of its weight (Martha et al., 2022). Si is used in multiple applications, including in glass, porcelain, silica gels, cement, concrete, silicone rubber, ceramics, and as alloying element with metals (Benavides et al., 2015). Over the past decade, Si has been used extensively in solar panels and electronic devices because of its advantageous properties (Salah et al., 2021; Wen et al., 2013).

With respect to LIBs, Si has gained substantial attention as an anode alternative due to its various favorable properties over commonly used graphite anodes. These include: (a) Low cost due to its abundance; (b) Highest theoretical storage capacity among all known materials (4200 mAh/g), which is significantly higher than the capacity of graphite (372 mAh/g) (Table 4); (c) Relatively low discharge potential (~0.4 V) over Li^+/Li, which helps to achieve higher battery energy density while avoiding two standard issues with graphite anodes – lithium plating and dendrite formation during lithiation; (d) Better chemical stability; (e) Good environmental compatibility; and (f) Low toxicity (Feng et al., 2018; Salah et al., 2019; Wen et al., 2013; Zuo et al., 2017). Further, research has shown the scope of Si use as a battery anode in a variety of forms, including as nanowires, thin films, nanocomposites, and also with dopants (Salah et al., 2021, 2019; Wen et al., 2013; Zuo et al., 2017).

Table 5 provides a detailed list of these forms. Together, these attributes make Si attractive as a battery anode material, despite the challenges associated with its use for commercial LIBs, such as its large volumetric expansion during lithiation and de-lithiation that reduces battery life and its low electrical conductivity that affects battery power density (Feng et al., 2018; Salah et al., 2021, 2019; Wen et al., 2013; Zuo et al., 2017).

Table 4: Electrochemical Properties of LIB Anodes – A Comparison (Hasa and Passerini, 2022)

LIB Anode Material	Lithiated phase	Gravimetric capacity (mAh/g)	Volumetric capacity (mAh/cm^3)	Average potential (V) v/s Li^+/Li	Density (g/cm^3)
Lithium	Li	3,862	2,047	0	0.53
Graphite	LiC_6	372	837	0.05	2.25
Lithium titanate ($Li_4Ti_5O_{12}$)	$Li_4Ti_5O_{12}$	175	613	1.6	3.5
Silicon	$Li_{4.4}Si$	4,200	9,786	0.4	2.3

Table 5: Silicon (Si) Forms Used in LIB Anodes (reproduced from (Zuo et al., 2017))

Forms	More details/Sub-forms	Examples
Polysiloxanes	SiOC	Si_zC_{1-z}, Si-O-C
Nanocomposites		Si/X (X = C, TiN)
	0-D Si/1-D carbon composites	Si/CNT
	0-D Si/2-D carbon composites	Si/graphene, Si/RGO (reduced graphite oxide), Si/graphene foam, Graphene/Si/carbon
	0-D Si/3-D Carbon composites	Si/porous C, core/shell Si/C
Alloys	Pure alloys	Mg_2Si, NiSi, SiAg, $CaSi_2$
	Alloy composites	$Fe_{20}Si_{80}$-graphite, FeSi/graphite, $FeSi_6$/graphite, SiNi/graphite, Mg_2Si/C, Si/NiTi, Si/$FeSi_2Ti$
	Alloy composites with 3D structure	Porous $NiSi_2$/Si/carbon
Si films	Si films	Films of varying thickness (250 nm to 1.1 μm)
	Si/composite films	Si/TiN, Fe/Si multilayer, Si nanowire assay film, CNT/Si, Si/Al
	Si/composite films + 3D structure	Patterned Si, Si-Cu-Ti with Cu_3Ti nanowires, Si-C/graphene (porous carbon, graphene layers)
Composites		Si/X (X = Ag, Cu)
Nanowires (NW) and Nanotubes (NT)	Si NW	Si, tin-seeded Si
	Si NW/composite	C-Si core-shell NW , carbon-coated Si NW, element-coated Si (element = Cu, Sn, Ag), Si/graphene
	NT	Si NT, sealed Si NT, carbon/CNT-coated Si, CNT-coated Si
3D Si	3D Si	Porous bulk Si, nest-like Si particles, nano-porous bulk Si, hollow Si nanospheres
	Composites	Ag-coated 3D/porous Si, carbon-coated microporous/multi-dimensional Si, X-coated Si (X = Cu, $TiSi_2$)
Multi-component systems		Nanocluster SiO_x-C composites, nano-Si/SiO_x/graphite composite, Si-SiO-SiO_2, Si NT-based, Fe-Cu-Si ternary composite
0-D/1-D/2-D/3-D: Zero/One/Two/Three-Dimensional		

Official data on the United States' production and consumption of Si metal are not available. However, the USGS does report data on combined domestic production of both ferrosilicon and Si metal, totaling 277,000 metric tons in 2020 and 310,000 metric tons in 2021 (USGS, 2022). This amounts to ~58% and ~68% respectively of U.S's Si usage in these forms (USGS, 2022), with the imports mostly from Brazil, Canada, Norway, Taiwan, Australia, China, and Germany. However, silicon is not always used directly in metallurgical form, but is often converted to subsequent forms for various applications, especially in the electrical and photovoltaic sectors. Frischknecht et al. (2020a) has highlighted a non-existent share of Si production in these forms in the United States. A further breakout on this aspect is not available.

2.2.2 Silicon Anode Manufacturing

Si metal is produced from silica and subjected to various processes to produce Si wafers for the various photovoltaic and electronic applications (Benavides et al., 2015; Frischknecht et al., 2020b). Figure 3 reproduces the schematic for Si wafer production from (Benavides et al., 2015). While extremely high levels of Si purity are needed for wafers, such demanding levels of purity may not be needed for LIB anodes (Benavides et al., 2015). Hence, we assume that only the initial two processes – production of metallurgical-grade Si from silica sand, and modified Siemens process – are needed to produce Si anodes desired for LIBs – like in the previous versions of GREET model (Benavides et al., 2015).

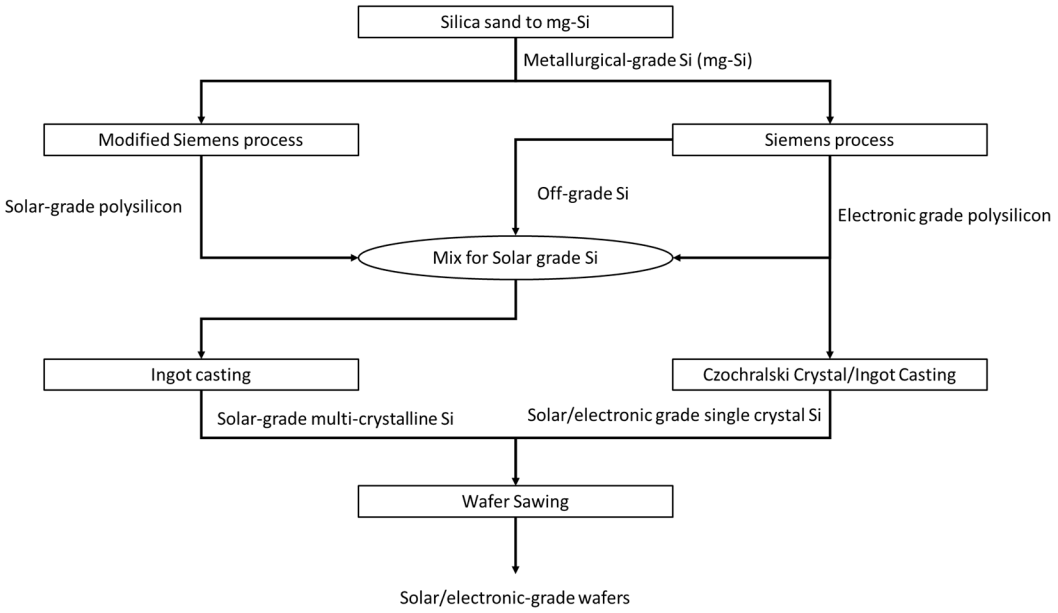

Figure 3: Schematic for Si Wafer Production (reproduced from (Benavides et al., 2015))

The process description for Si anode/wafer production remains the same as that given in Argonne's earlier report on this subject (Benavides et al., 2015). Briefly, metallurgical-grade Si is produced via carbothermal reduction of silica in an electric furnace. Carbon sources used in

this process are coal, coke, wood chips, and/or charcoal (Frischknecht et al., 2020b). This metallurgical-grade Si is then treated in the modified Siemens process to produce solar-grade polysilicon, which is assumed to be the same as the Si anode used in LIBs.

Note that Si is used in a variety of forms as anodes in LIBs (Table 5), requiring this solar-grade Si from the modified Siemens process to be converted to these forms through additional process routes for use as anodes. However, data on material and energy flows of such conversion processes are based on laboratory-scale processes (discussed in the next sub-section), and may not always reflect the likely changes in these flows at commercial scale production. Hence, this conversion step and its associated inventory are not considered in the material and energy flows for Si anodes in the updated GREET model.

2.2.3 Material & Energy Flows for Silicon Anode Production

For the initial two processes in Figure 3 (metallurgical-grade Si production and modified Siemens process), we use material and energy flows from the same reference (Frischknecht et al., 2020b) as that for Si wafer production in the updated GREET model. Frischknecht et al., (2020b) provides these flows for Si production at four locations (US/North America, China, Asia & Pacific, Europe) and their respective shares in total Si output from various processes shown in Figure 3. In the case of metallurgical-grade Si, we combine Si production from these four regions as per their respective shares in the United States' total silicon consumption: US (58%), Europe (6.4%), China (2.5%) and the remaining from Asia & Pacific (APAC) region (USGS, 2022). However, for all other stages such as solar-grade production, Frischknecht et al., (2020b) reports that the entire U.S. consumption is met by China. Hence, material and energy flows related to Chinese production are used for solar-grade silicon.

Literature indicates that Si obtained from the modified Siemens process has to be processed further to obtain it in the desired form for use in LIBs (Table 5) (Zuo et al., 2017). Our literature review highlighted two studies that provide material and energy flows (LCIs) for two such Si anode forms: silicon nanowires or SiNWs (Li et al., 2014) and silicon nanotubes or SiNTs (Deng et al., 2019). A brief description of their respective processing techniques is given below.

Li et al. (2014) trace the production of SiNWs all the way from silica flour (sand). In their study, 325-mesh Si powder is produced from silica flour through a series of processes to obtain Si powders. These include: (a) Carbothermal reduction; (b) Chemical purification (combines fluid bed combustion, distillation, and chemical vapor deposition); and (c) Ball milling. Subsequently, this 325-mesh Si powder is transformed to SiNWs using various chemical reagents, such as nitric acid, ammonium hydroxide, acetone, ethanol, hydrogen fluoride, hydrogen peroxide, and silver nitrate. The final output also contains silver and silicon wastes, as well as large amounts of solution waste due to the use of multiple liquid reagents in considerable amounts.

Deng et al. (2019) provide a description of SiNT synthesis at laboratory-scale. Surfactant (ethoxylated alcohol) is mixed and stirred with cyclohexane, hydrazine hydrate, and nickel

chloride to produce nickel chloride-hydrazine compound in a nano-rod template structure. Next, diethylamine and tetraethyl orthosilicate (TEOS) are added to this solution under stirring, and TEOS hydrolyzes to form silica coating on the nano-rods. Upon a few more hours of stirring, the solution is etched with hydrochloric acid to remove the nano-rod templates. These templates are centrifuged and washed further to obtain SiNTs, which are further purified via combustion at 700°C and reduction using magnesium (with a 32% conversion ratio). The obtained tubes are centrifuged in multiple rounds using distilled water to yield high-purity SiNT anodes.

Both Li et al. (2014) and Deng et al. (2019) provide detailed material and energy flows regarding the production of their respective Si anode forms, and these flows have also been used to evaluate the effects of Si anodes in other studies (Wu and Kong, 2018). However, while Li et al. (2014) provides these flows for laboratory-scale production of Si anode (SiNW), Deng et al. (2019) has estimated their inventory from laboratory-scale production. Hence, these LCIs may not be entirely representative of commercial-scale production of these anodes and the associated possibilities such production may hold for efficiency improvements. This is also stated in Deng et al. (2019), who highlight the scope for such efficiency improvements in both magnesium-based reduction of SiNTs and in cyclohexane consumption for SiNT processing. Hence, we have not incorporated either of these two LCIs in the updated GREET model. But we provide their description to highlight the advancement potentials that may be on the horizon for battery technology.

Table 6 provides the material and energy flows for both metallurgical-grade Si production and the modified Siemens process, as obtained from Frischknecht et al. (2020b), and included in the updated GREET model. All these inputs are provided in the Solar photovoltaic sheet of GREET2.

Table 6: Material and Energy Flows for Silicon Anode Production (obtained from (Frischknecht et al., 2020b)**)**

Inputs	**Metallurgical grade silicon**				**Solar grade silicon**
	US	**China**	**APAC**	**Europe**	**China**
Material consumption of each process: lb per lb product					
Sodium Hydroxide					0.870
Calcium Carbonate					0.580
Oxygen	0.020	0.020	0.020	0.020	
Silica	2.700	2.680	2.700	2.700	0.000
Graphite	0.100	0.120	0.100	0.100	0.000
US: Metallurgical grade silicon					0.000
China: Metallurgical grade silicon					1.120
APAC: Metallurgical grade silicon					0.000
Europe: Metallurgical grade silicon					0.000
Chlorine					0.200

Table 6 (Cont.)

Inputs	Metallurgical grade silicon				Solar grade silicon
	US	China	APAC	Europe	China
Energy consumption of each process: mmbtu per lb product					
Electricity from grid mix	0.01702	0.01935	0.017	0.017	0.086
Natural gas					0.015
Char	0.002	0.000	0.002	0.002	
Coke	0.010	0.012	0.010		
Petcoke	0.007	0.008	0.007	0.007	
Liquid hydrogen					0.003

2.3 Lithium Anodes

2.3.1 Availability & Significance

Lithium (Li) is already a major constituent of LIBs, used primarily in the form of battery-grade lithium carbonate (Li2CO3) and lithium hydroxide (LiOH.H2O) to produce LIB cathodes (Dai et al., 2019; Dunn et al., 2015). However, Li is also considered as an excellent alternative to conventional graphite anodes due to its comparatively favorable properties. These include: (a) Extremely high theoretical specific capacity (see Table 4); (b) Potential to accomplish higher battery energy density than for LIBs with graphite and Si anodes; (c) Low metal density; and (d) Lowest negative electrochemical potential (-3.04 V) of all anodes vis-à-vis the standard hydrogen electrode (Wang et al., 2020; Yasin et al., 2022; Zhang et al., 2020). Also, apart from Li anodes being an alternative to graphite for LIBs, they are also important as anodes for other types of batteries, such as lithium-sulfur (Li-S) and lithium-air (Li-A) batteries that are considered as the next generation of batteries (Imanishi and Yamamoto, 2019; Mahandra et al., 2022; Tan et al., 2017). Hence, despite the challenges of dendrite formation, electrolyte consumption through auto-reaction with Li, and mechanical instabilities (such as the fracture of solid electrolyte interphase layer) that lower battery Coulombic efficiency (Ghazi et al., 2019; Wang et al., 2020; Yasin et al., 2022; Zhang et al., 2020), Li has gained increasing attention in the battery research community for its anode-related prospects.

The United States produces limited amounts of lithium as Li compounds (Li_2CO_3, LiOH, and LiCl), with Albemarle and Livent being the major players in this domain (Rapier, 2020; USGS, 2022). These materials are produced from brine resources imported from Chile into the US (USGS, 2022).

2.3.2 Lithium Anode Manufacturing

Figure 4 shows a schematic for production of Li anodes, reproduced from Argonne's prior report on material and energy flows to produce LIB cathodes and anodes (Dunn et al., 2015). The detailed production process for Li anodes is already given in that report, so we only provide a summary of it here.

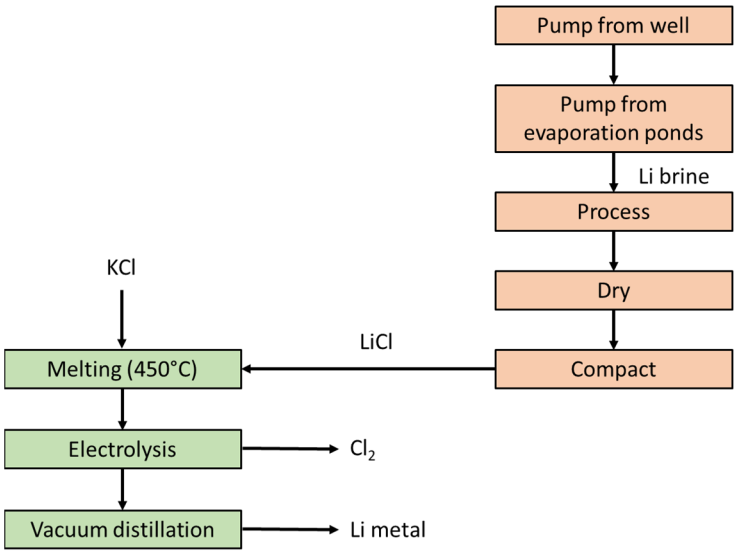

Figure 4: Schematic for Li-anode production (reproduced from (Dunn et al., 2015))

Li brine, pumped from reserves and evaporated in ponds, crystallizes in these ponds, and is then processed, dried, and compacted to produce lithium chloride (LiCl). LiCl is melted in the presence of potassium chloride (KCl) and electrolyzed at ~ 450°C to produce lithium (and chlorine). The Li obtained here has high purity (97-99.5%), but it may need further purification to be suitable for use as anode. If such high purity is needed (on which literature does not lend clarity), it is attained typically through vacuum distillation in an electric chamber at 600-800°C to vaporize away the impurities, leaving behind the desired high-purity Li metal.

2.3.3 Material and Energy Flows for Lithium Anode Production

A few studies exist on the LCA of batteries with Li anodes (Deng et al., 2017; Wu and Kong, 2018). However, these studies do not provide detailed inventory (material and energy flows) for the different processes associated with Li metal production (shown in Figure 4), nor could other studies with such data be found in our literature review. Hence, no changes are made to these flows in the updated GREET model, and they remain the same as those provided in Argonne's previous report on this subject (Dunn et al., 2015).

3 NEW BATTERY MATERIALS AND CHEMISTRIES

LIBs have remained the most favored battery technology for EVs over the past few decades due to their various advantages. However, there also exist concerns regarding a number of issues and challenges associated with LIBs. These include: (a) Limits on battery energy density amidst the desire to boost EV driving range under a variety of geographic regions and climates; (b) Reduced availability of LIB cathode constituent materials over time, such as nickel, lithium (Li), and cobalt (Co); and (c) Structure and performance-related instabilities over the operational life of batteries through their use of specific constituents, such as dendrite formation associated with graphitic (and also Li metal) anodes (Deng et al., 2017; Ding et al., 2019; Speirs et al., 2014). Hence, researchers have been focusing on developing alternatives to both specific LIB constituents and to LIBs itself.

Regarding anode materials, apart from silicon and lithium, another alternative considered is lithium titanate (LTO) due to multiple advantages. These include its: (a) Stable spinel structure that does not exhibit any strain during lithiation/de-lithiation process, thus enabling fast charging and discharging; (b) High working potential (Table 4) that helps to avoid dendrite formation and solid electrolyte interphase layer formation on electrode surface, and thus improves battery safety; (c) Ultra-long cycle lifetime (up to 20,000 cycles – or 10 times higher than that of graphite); and (d) Ability to operate under a wide range of temperature conditions (-30 to 60°C) at high capacities (Ding et al., 2019). Admittedly, challenges exist in the commercial use of LTO anodes in LIBs for EVs, such as their low electric conductivity and limited Li diffusion capacity that can limit rapid charging/discharging over longer time durations, and the need to use high-voltage cathode materials to match LTO's high potential (Ding et al., 2019). However, with researchers working on addressing these challenges (Ding et al., 2019) and given its inherent advantages, LTO remains a potential alternative future anode. In this update of GREET, LTO is not considered for two reasons: (a) Lack of its inventory in our literature review; and (b) Non-inclusion of LTO as an anode in Argonne's Battery Performance and Cost (BatPaC) 5.0 model, which informs the battery material composition used in GREET for computing battery-related environmental impacts. Future efforts will explore the possibility of incorporating this anode in GREET model and comparing the impacts of LIBs using it with those based on both conventional graphite and alternative silicon and lithium-metal anodes.

Regarding alternatives to LIBs, these depend on the application of concern. For the EV sector, three battery systems stand out for their potential use in the future: lithium-sulfur (Li-S), lithium-air (Li-A), and all-solid-state batteries (SSBs) (Ding et al., 2019). We give below a brief description of the respective characteristics of each of these battery systems below.

Li-S batteries typically consist of a sulfur cathode, Li metal anode, and an organic electrolyte – similar to LIBs (Mahandra et al., 2022; Zhao et al., 2020). The combination of sulfur cathode and Li anode is used as this results in higher battery energy density of Li-S batteries (2,600 Wh/kg) (Mahandra et al., 2022). Moreover, the abundance of sulfur makes it both less expensive and less toxic compared to LIBs (Glossmann et al., 2022; Mahandra et al., 2022; Zhao et al., 2020; Zheng et al., 2022). Through these properties, Li-S batteries offer the scope to lower weight and enhance driving range of EVs, while also offering the possibility for

flexible storage of solar energy for various applications in the domestic (residential), military, and marine sectors (Mahandra et al., 2022). Challenges that currently hinder the commercialization of Li-S batteries include: (a) Deterioration in their capacity over time through the degradation of cell components; (b) Formation of shorter polysulfides via reaction of long-chain polysulfides with anode, which then diffuse to the cathode and corrode it, reducing the battery Coulombic efficiency over time; (c) Solubility of active species (when sulfur reacts with lithium to precipitate out) – that increases the battery's internal resistance and causes a loss in active material mass; and (d) Variation in battery discharge characteristics when compared with LIBs, which needs to be understood through detailed studies (Mahandra et al., 2022; Zhao et al., 2020; Zheng et al., 2022). Future research on these issues is expected to enable Li-S batteries to become commercially viable for EV application.

Li-A batteries are different from both LIBs and Li-S batteries, as they are connected to the atmosphere (source of oxygen supply) to operate (Farooqui et al., 2017; Imanishi and Yamamoto, 2019; Tan et al., 2017). These batteries contain Li anodes that react with oxygen from air, with their capacity limited theoretically by the anode (Imanishi and Yamamoto, 2019; Tan et al., 2017). This air cathode is the most important part of Li-A batteries, and the access to air makes this battery theoretically more renewable and material-secure than LIBs from the perspective of cathodes (Dobley, 2013; Farooqui et al., 2017). Further, Li-A batteries offer longer storage lives, high operating voltages, a flat discharge voltage profile, highest theoretical specific energy (11,860 Wh/kg), recyclable cell components, and potential for rechargeability (Dobley, 2013; Farooqui et al., 2017; Imanishi and Yamamoto, 2019; Tan et al., 2017). However, just like Li-S batteries, Li-A batteries too are affected by a number of challenges. These include the need to protect the cathode from water and carbon dioxide, issues with electrolytes that can lower the permeation of oxygen into these batteries, lithium corrosion due to air moisture or use of aqueous electrolytes, and the need to avoid lithium dendrite formation, among others (Dobley, 2013; Farooqui et al., 2017; Imanishi and Yamamoto, 2019; Tan et al., 2017). However, researchers are working on various solutions to address these challenges and enable Li-A battery commercialization for EVs (Farooqui et al., 2017; Imanishi and Yamamoto, 2019).

Lastly, SSBs are another exciting alternative with the potential to replace LIBs in automotive applications (Ding et al., 2019). SSBs avoid the flammable organic liquid electrolytes in LIBs with a solid non-flammable electrolyte, which in turn avoids the complex reactions at the solid/liquid interfaces in LIBs and the related thermal instability, making them superior to LIBs (Ding et al., 2019; Kamaya et al., 2011; M. J. Wang et al., 2021). SSBs use a variety of solid-state electrolytes, such as argyrodites, polymers, oxides, sulfides, and thin films, with oxides and sulfides being the preferred choices (Ding et al., 2019). Moreover, SSBs are expected to be safer, have longer cycle life and higher energy density, and have fewer packaging and state-of-charge monitoring requirements (Ding et al., 2019). The solid electrolytes of SSBs are also expected to act as separators as well as enable cell stacking in a single package without the risk of ionic short-circuit, thus boosting the battery specific energy by cutting down on empty volume between single cells (Ding et al., 2019). From a material perspective, these are often used with Li anodes, which can help to improve battery capacities. Moreover, SSBs can be used with the same cathodes as those used in LIBs with good battery performance, eliminating the need to develop new cathodes for these battery systems.

REFERENCES

Agubra, V., Fergus, J., 2013. Lithium Ion Battery Anode Aging Mechanisms. Mater. 2013, Vol. 6, Pages 1310-1325 6, 1310–1325. https://doi.org/10.3390/MA6041310

Asaithambi, G., Treiber, M., Kanagaraj, V., 2019. Life Cycle Assessment of Conventional and Electric Vehicles. Int. Clim. Prot. 161–168. https://doi.org/10.1007/978-3-030-03816-8_21

Asenbauer, J., Eisenmann, T., Kuenzel, M., Kazzazi, A., Chen, Z., Bresser, D., 2020. The success story of graphite as a lithium-ion anode material – fundamentals, remaining challenges, and recent developments including silicon (oxide) composites. Sustain. Energy Fuels 4, 5387–5416. https://doi.org/10.1039/D0SE00175A

Benavides, P.T., Dai, Q., Sullivan, J.L., Kelly, J.C., Dunn, J.B., 2015. Material and Energy Flows Associated with Select Metals in GREET 2. Molybdenum, Platinum, Zinc, Nickel, Silicon (No. ANL/ESD-15/11). Argonne, IL (United States). https://doi.org/10.2172/1224976

Bennett, A., 2021. The critical need for synthetic and natural graphite to meet EV sector growth [WWW Document]. Fastmarkets. URL https://www.fastmarkets.com/insights/the-critical-need-for-synthetic-and-natural-graphite-to-meet-ev-sector-growth (accessed 7.15.22).

Bhatuda, G., 2021. Visualizing the Natural Graphite Supply Problem [WWW Document]. Elements. URL https://elements.visualcapitalist.com/visualizing-the-natural-graphite-supply-problem/ (accessed 7.15.22).

Bogacki, M., Oleniacz, R., Mazur, M., 2010. Evaluation of gas emissions from graphitising of carbon products, in: Heim, A., Tomalczyk, M., Bartczak, Z. (Eds.), Environmental Engineering III. CRC Press, pp. 23–28. https://doi.org/10.1201/B10566-7

Bogacki, M., Oleniacz, R., Mazur, M., Szczyglowski, P., 2012. Air pollution emissions during baking of semi-finished graphite products in a tunnel furnace. Environ. Prot. Eng. 38, 15–23.

CoP26, 2021. UN Climate Change Conference (COP26) – Glasgow 2021 [WWW Document]. UN Clim. Chang. Conf. UK 2021 (In Partnersh. with Italy). URL https://ukcop26.org/ (accessed 11.16.21).

Dai, Q., Kelly, J.C., Gaines, L., Wang, M., 2019. Life Cycle Analysis of Lithium-Ion Batteries for Automotive Applications. Batter. 2019, Vol. 5, Page 48 5, 48. https://doi.org/10.3390/BATTERIES5020048

Daimer, J., 2021. 6.2 Manufacturing*, in: Jäger, H., Frohs, W. (Eds.), Industrial Carbon and Graphite Materials, Volume I. John Wiley & Sons, Ltd, pp. 214–229. https://doi.org/10.1002/9783527674046.CH6_2

Deng, Y., Li, J., Li, T., Gao, X., Yuan, C., 2017. Life cycle assessment of lithium sulfur battery for electric vehicles. J. Power Sources 343, 284–295. https://doi.org/10.1016/j.jpowsour.2017.01.036

Deng, Y., Ma, L., Li, T., Li, J., Yuan, C., 2019. Life Cycle Assessment of Silicon-Nanotube-Based Lithium Ion Battery for Electric Vehicles. ACS Sustain. Chem. Eng. 7, 599–610.

https://doi.org/10.1021/ACSSUSCHEMENG.8B04136/ASSET/IMAGES/LARGE/SC-2018-04136W_0007.JPEG

Ding, Y., Cano, Z.P., Yu, A., Lu, J., Chen, Z., 2019. Automotive Li-Ion Batteries: Current Status and Future Perspectives. Electrochem. Energy Rev. 2019 21 2, 1–28. https://doi.org/10.1007/S41918-018-0022-Z

Dobley, A., 2013. Catalytic Batteries, in: Suib, S.L. (Ed.), New and Future Developments in Catalysis: Batteries, Hydrogen Storage and Fuel Cells. Elsevier, pp. 1–16. https://doi.org/10.1016/B978-0-444-53880-2.00001-6

Dolganova, I., Rödl, A., Bach, V., Kaltschmitt, M., Finkbeiner, M., 2020. A Review of Life Cycle Assessment Studies of Electric Vehicles with a Focus on Resource Use. Resour. 2020, Vol. 9, Page 32 9, 32. https://doi.org/10.3390/RESOURCES9030032

Dunn, J., James, C., Gaines, L., Gallaghar, K., Dai, Q., Kelly, J., 2015. Material and Energy Flows in the Production of Cathode and Anode Materials for Lithium Ion Batteries (No. ANL/ESD-14/10 Rev). Argonne, IL. https://doi.org/10.2172/1224963

Dunn, J.B., Gaines, L., Kelly, J.C., James, C., Gallagher, K.G., 2014. The significance of Li-ion batteries in electric vehicle life-cycle energy and emissions and recycling's role in its reduction. Energy Environ. Sci. 8, 158–168. https://doi.org/10.1039/C4EE03029J

Engels, P., Cerdas, F., Dettmer, T., Frey, C., Hentschel, J., Herrmann, C., Mirfabrikikar, T., Schueler, M., 2022. Life cycle assessment of natural graphite production for lithium-ion battery anodes based on industrial primary data. J. Clean. Prod. 336, 130474. https://doi.org/10.1016/J.JCLEPRO.2022.130474

Farooqui, U.R., Ahmad, A.L., Hamid, N.A., 2017. Challenges and potential advantages of membranes in lithium air batteries: A review. Renew. Sustain. Energy Rev. 77, 1114–1129. https://doi.org/10.1016/J.RSER.2016.11.220

Feng, K., Li, M., Liu, W., Ghorbani Kashkooli, A., Xiao, X., Cai, M., Chen, Z., Feng, K., Li, M., Liu, W., Kashkooli, A.G., Chen, Z., Xiao, X., Cai, M., 2018. Silicon-Based Anodes for Lithium-Ion Batteries: From Fundamentals to Practical Applications. Small 14, 1702737. https://doi.org/10.1002/SMLL.201702737

Frischknecht, R., Stolz, P., Krebs, L., de Wild-Scholten, M., Sinha, P., 2020a. Life Cycle Inventories and Life Cycle Assessments of Photovoltaic Systems 2020.

Frischknecht, R., Stolz, P., Krebs, L., de Wild-Scholten, M., Sinha, P., Fthenakis, V., Kim, H.C., Raugei, M., Stucki, M., 2020b. Life Cycle Inventories and Life Cycle Assessment of Photovoltaic Systems.

Gao, S., Gong, X., Liu, Y., Zhang, Q., 2018. Energy Consumption and Carbon Emission Analysis of Natural Graphite Anode Material for Lithium Batteries. Mater. Sci. Forum 913, 985–990. https://doi.org/10.4028/www.scientific.net/MSF.913.985

Ghazi, Zahid Ali, Sun, Z., Sun, C., Qi, F., An, B., Li, Feng, Cheng, Hui-Ming, Ghazi, Z A, Sun, Z.H., Sun, C.G., Qi, F.L., Li, F, Cheng, H.-M, An, B.G., 2019. Key Aspects of Lithium Metal Anodes for Lithium Metal Batteries. Small 15, 1900687. https://doi.org/10.1002/SMLL.201900687

Glossmann, T., Raj, A., Pajan, T., Buch, E., 2022. Introduction to the lithium-sulfur system:

Technology and electric vehicle applications, in: Kumta, P.N., Hepp, A.F., Datta, M.K., Velikokhatnyi, O.I. (Eds.), Lithium-Sulfur Batteries: Advanced in High-Energy Density Batteries. Elsevier, pp. 3–15. https://doi.org/10.1016/B978-0-12-819676-2.00010-4

Graphite Corp., 2021. Graphite is an excellent anode material for lithium batteries [WWW Document]. Graph. Corp. URL https://www.graphite-corp.com/materials/Graphite-is-an-excellent-anode-material-for-lithium-batteries-4.html (accessed 7.15.22).

Hao, L., Bonan, L., Geng, C., Jieyun, Z., Fei, L., Xinping, Q., Hui, L., Fang, L., Suning, F., Wei, C., Hong, L., Liquan, C., 2016. Technology review of anode materials for lithium ion batteries. Energy Storage Sci. Technol. 5, 119. https://doi.org/10.3969/J.ISSN.2095-4239.2016.02.001

Hasa, I., Passerini, S., 2022. Silicon anode systems for lithium-ion batteries, in: Kumta, P.N., Hepp, A.F., Datta, M.K., Velikokhatnyi, O.I. (Eds.), Silicon Anode Systems for Lithium-Ion Batteries. Elsevier, pp. 3–46. https://doi.org/10.1016/B978-0-12-819660-1.00002-5

Hellweg, S., Milà i Canals, L., Canals, L.M. i, 2014. Emerging approaches, challenges and opportunities in life cycle assessment. Science 344, 1109–13. https://doi.org/10.1126/science.1248361

Imanishi, N., Yamamoto, O., 2019. Perspectives and challenges of rechargeable lithium–air batteries. Mater. Today Adv. 4, 100031. https://doi.org/10.1016/J.MTADV.2019.100031

Jara, A.D., Betemariam, A., Woldetinsae, G., Kim, J.Y., 2019. Purification, application and current market trend of natural graphite: A review. Int. J. Min. Sci. Technol. 29, 671–689. https://doi.org/10.1016/J.IJMST.2019.04.003

Kamaya, N., Homma, K., Yamakawa, Y., Hirayama, M., Kanno, R., Yonemura, M., Kamiyama, T., Kato, Y., Hama, S., Kawamoto, K., Mitsui, A., 2011. A lithium superionic conductor. Nat. Mater. 2011 109 10, 682–686. https://doi.org/10.1038/nmat3066

Kelly, J.C., Dai, Q., Wang, M., 2019. Globally regional life cycle analysis of automotive lithium-ion nickel manganese cobalt batteries. Mitig. Adapt. Strateg. Glob. Chang. 2019 253 25, 371–396. https://doi.org/10.1007/S11027-019-09869-2

Kelly, J.C., Elgowainy, A., Isaac, R., Ward, J., Islam, E., Rousseau, A., Sutherland, I., Wallington, T.J., Alexander, M., Muratori, M., Franklin, M., Adams, J., Rustagi, N., 2022. Cradle-to-Grave Lifecycle Analysis of U.S. Light-Duty Vehicle-Fuel Pathways: A Greenhouse Gas Emissions and Economic Assessment of Current (2020) and Future (2030-2035) Technologies (No. ANL-22/27). Argonne, IL (United States). https://doi.org/10.2172/1875764

Lai, X., Chen, Q., Tang, X., Zhou, Y., Gao, F., Guo, Y., Bhagat, R., Zheng, Y., 2022. Critical review of life cycle assessment of lithium-ion batteries for electric vehicles: A lifespan perspective. eTransportation 12, 100169. https://doi.org/10.1016/J.ETRAN.2022.100169

Li, B., Gao, X., Li, J., Yuan, C., 2014. Life cycle environmental impact of high-capacity lithium ion battery with silicon nanowires anode for electric vehicles. Environ. Sci. Technol. 48, 3047–3055. https://doi.org/10.1021/ES4037786/SUPPL_FILE/ES4037786_SI_002.PDF

Mahandra, H., Alvial-Hein, G., Sharifidarabad, H., Faraji, F., Singh, O., 2022. Recent developments in lithium–sulfur batteries, in: Gupta, R.K., Nguyen, T.A., Song, H., Yasin, G. (Eds.), Lithium-Sulfur Batteries. Elsevier, pp. 11–36. https://doi.org/10.1016/B978-0-

323-91934-0.00024-7

Martha, S.K., Elias, L., Ghosh, S., 2022. Nanostructured 3D (three dimensional) electrode architectures of silicon for high-performance Li-ion batteries. Silicon Anode Syst. Lithium-Ion Batter. 331–371. https://doi.org/10.1016/B978-0-12-819660-1.00013-X

Northern Graphite, 2021. Natural Graphite: The Material for a Green Economy [WWW Document]. Elements. URL https://elements.visualcapitalist.com/natural-graphite-the-material-for-a-green-economy/ (accessed 7.15.22).

Olivetti, E.A., Ceder, G., Gaustad, G.G., Fu, X., 2017. Lithium-Ion Battery Supply Chain Considerations: Analysis of Potential Bottlenecks in Critical Metals. Joule 1, 229–243. https://doi.org/10.1016/J.JOULE.2017.08.019

Pillot, C., 2019. The Rechargeable Battery Market and Main Trends 2018-2030 [WWW Document]. Avicenne Energy.

Qatar Green Leaders, 2019. Supply Chain Looms as Serious Threat to Batteries' Green Reputation [WWW Document]. Qatar Green Leaders. URL https://qatargreenleaders.com/news/sustainability-news/4310-supply-chain-looms-as-serious-threat-to-batteries-green-reputation (accessed 7.15.22).

Rapier, R., 2020. The World's Top Lithium Producers [WWW Document]. Forbes. URL https://www.forbes.com/sites/rrapier/2020/12/13/the-worlds-top-lithium-producers/?sh=3fb6b3945bc6 (accessed 7.15.22).

Rui, X., Geng, Y., Zhuang, M., Xiao, S., Sun, X., 2022. Emergy-based environmental accounting of graphite anode material production. J. Clean. Prod. 339, 130705. https://doi.org/10.1016/J.JCLEPRO.2022.130705

Salah, M., Hall, C., Murphy, P., Francis, C., Kerr, R., Stoehr, B., Rudd, S., Fabretto, M., 2021. Doped and reactive silicon thin film anodes for lithium ion batteries: A review. J. Power Sources 506, 230194. https://doi.org/10.1016/J.JPOWSOUR.2021.230194

Salah, M., Murphy, P., Hall, C., Francis, C., Kerr, R., Fabretto, M., 2019. Pure silicon thin-film anodes for lithium-ion batteries: A review. J. Power Sources 414, 48–67. https://doi.org/10.1016/J.JPOWSOUR.2018.12.068

Shafique, M., Luo, X., 2022. Environmental life cycle assessment of battery electric vehicles from the current and future energy mix perspective. J. Environ. Manage. 303, 114050. https://doi.org/10.1016/J.JENVMAN.2021.114050

Speirs, J., Contestabile, M., Houari, Y., Gross, R., 2014. The future of lithium availability for electric vehicle batteries. Renew. Sustain. Energy Rev. 35, 183–193. https://doi.org/10.1016/J.RSER.2014.04.018

Stringfellow, W.T., Dobson, P.F., 2021. Technology for the Recovery of Lithium from Geothermal Brines. Energies 2021, Vol. 14, Page 6805 14, 6805. https://doi.org/10.3390/EN14206805

Surovtseva, D., Crossin, E., Pell, R., Stamford, L., 2022. Toward a life cycle inventory for graphite production. J. Ind. Ecol. 26, 964–979. https://doi.org/10.1111/JIEC.13234

Tan, P., Jiang, H.R., Zhu, X.B., An, L., Jung, C.Y., Wu, M.C., Shi, L., Shyy, W., Zhao, T.S.,

2017. Advances and challenges in lithium-air batteries. Appl. Energy 204, 780–806. https://doi.org/10.1016/J.APENERGY.2017.07.054

Toba, A.L., Nguyen, R.T., Cole, C., Neupane, G., Paranthaman, M.P., 2021. U.S. lithium resources from geothermal and extraction feasibility. Resour. Conserv. Recycl. 169, 105514. https://doi.org/10.1016/J.RESCONREC.2021.105514

US DoE, 2011. Critical Materials Strategy. Washington DC.

US DOE, 2020. Critical Minerals and Materials: U.S. Department of Energy's Strategy to Support Domestic Critical Mineral and Material Supply Chains (FY 2021-FY 2031). Washington DC. https://doi.org/10.3133/70194932

USGS, 2022. Mineral Commodity Summaries 2022, Mineral Commodity Summaries. Reston. https://doi.org/10.3133/MCS2022

Verma, S., Dwivedi, G., Verma, P., 2022. Life cycle assessment of electric vehicles in comparison to combustion engine vehicles: A review. Mater. Today Proc. 49, 217–222. https://doi.org/10.1016/J.MATPR.2021.01.666

Vohler, O., Sturm, F. von, Wege, E., Frohs, W., 2021. Graphite*, in: Jäger, H., Frohs, W. (Eds.), Industrial Carbon and Graphite Materials, Volume I. John Wiley & Sons, Ltd, pp. 89–103. https://doi.org/10.1002/9783527674046.CH5

Wang, M., Elgowainy, A., Lee, U., Bafana, A., Banerjee, S., Benavides, P.T., Bobba, P., Burnham, A., Cai, H., Gracida-Alvarez, U.R., Hawkins, T.R., Iyer, R.K., Kelly, J.C., Kim, T., Kingsbury, K., Kwon, H., Li, Y., Liu, X., Lu, Z., Ou, L., Siddique, N., Sun, P., Vyawahare, P., Winjobi, O., Wu, M., Xu, H., Yoo, E., Zaimes, G.G., Zang, G., 2021. Summary of Expansions and Updates in GREET® 2021 (No. ANL/ESD-21/16). Lemont.

Wang, M.J., Kazyak, E., Dasgupta, N.P., Sakamoto, J., 2021. Transitioning solid-state batteries from lab to market: Linking electro-chemo-mechanics with practical considerations. Joule 5, 1371–1390. https://doi.org/10.1016/J.JOULE.2021.04.001

Wang, R., Cui, W., Chu, F., Wu, F., 2020. Lithium metal anodes: Present and future. J. Energy Chem. 48, 145–159. https://doi.org/10.1016/J.JECHEM.2019.12.024

Wen, Z., Lu, G., Mao, S., Kim, H., Cui, S., Yu, K., Huang, X., Hurley, P.T., Mao, O., Chen, J., 2013. Silicon nanotube anode for lithium-ion batteries. Electrochem. commun. 29, 67–70. https://doi.org/10.1016/J.ELECOM.2013.01.015

Winjobi, O., Kelly, J.C., Dai, Q., 2022. Life-cycle analysis, by global region, of automotive lithium-ion nickel manganese cobalt batteries of varying nickel content. Sustain. Mater. Technol. 32, e00415. https://doi.org/10.1016/J.SUSMAT.2022.E00415

Wu, Z., Kong, D., 2018. Comparative life cycle assessment of lithium-ion batteries with lithium metal, silicon nanowire, and graphite anodes. Clean Technol. Environ. Policy 20, 1233–1244. https://doi.org/10.1007/S10098-018-1548-9/FIGURES/6

Wu, Z., Wang, M., Zheng, J., Sun, X., Zhao, M., Wang, X., 2018. Life cycle greenhouse gas emission reduction potential of battery electric vehicle. J. Clean. Prod. 190, 462–470. https://doi.org/10.1016/J.JCLEPRO.2018.04.036

Yang, Y., Wu, S., Zhang, Y., Liu, C., Wei, X., Luo, D., Lin, Z., 2021. Towards efficient binders

for silicon based lithium-ion battery anodes. Chem. Eng. J. 406, 126807. https://doi.org/10.1016/J.CEJ.2020.126807

Yasin, G., Muhammad, N., Ibraheem, S., Kumar, A., Nguyen, T.A., Ibrahim, S., 2022. Lithium metal anode: an introduction, in: Gupta, R.K., Nguyen, T.A., Song, H., Yasin, G. (Eds.), Lithium-Sulfur Batteries. Elsevier, pp. 489–497. https://doi.org/10.1016/B978-0-323-91934-0.00010-7

Yin, E., Wong, C., Chi, D., Ho, K., So, S., Tsang, C.-W., Man, E., Chan, H., Wong, E.Y.C.;, Ho, D.C.K.;, 2021. Life Cycle Assessment of Electric Vehicles and Hydrogen Fuel Cell Vehicles Using the GREET Model—A Comparative Study. Sustain. 2021, Vol. 13, Page 4872 13, 4872. https://doi.org/10.3390/SU13094872

Zhang, H., Yang, Y., Ren, D., Wang, L., He, X., 2021. Graphite as anode materials: Fundamental mechanism, recent progress and advances. Energy Storage Mater. 36, 147–170. https://doi.org/10.1016/J.ENSM.2020.12.027

Zhang, Q., Gong, X., Meng, X., 2018. Environment Impact Analysis of Natural Graphite Anode Material Production. Mater. Sci. Forum 913, 1011–1017. https://doi.org/10.4028/www.scientific.net/MSF.913.1011

Zhang, Y., Zuo, T.T., Popovic, J., Lim, K., Yin, Y.X., Maier, J., Guo, Y.G., 2020. Towards better Li metal anodes: Challenges and strategies. Mater. Today 33, 56–74. https://doi.org/10.1016/J.MATTOD.2019.09.018

Zhao, M., Li, B.Q., Zhang, X.Q., Huang, J.Q., Zhang, Q., 2020. A Perspective toward Practical Lithium-Sulfur Batteries. ACS Cent. Sci. 6, 1095–1104. https://doi.org/10.1021/ACSCENTSCI.0C00449/ASSET/IMAGES/LARGE/OC0C00449_0005.JPEG

Zheng, Z., Xia, G., Ye, J., Fu, Z., Li, X., Biggs, M.J., Hu, C., 2022. Sustainability of lithium–sulfur batteries, in: Gupta, R.K., Nguyen, T.A., Song, H., Yasin, G. (Eds.), Lithium-Sulfur Batteries. Elsevier, pp. 603–626. https://doi.org/10.1016/B978-0-323-91934-0.00017-X

Zuo, X., Zhu, J., Müller-Buschbaum, P., Cheng, Y.-J.J., 2017. Silicon based lithium-ion battery anodes: A chronicle perspective review. Nano Energy 31, 113–143. https://doi.org/10.1016/j.nanoen.2016.11.013

Energy Systems and Infrastructure Analysis Division
Argonne National Laboratory
9700 South Cass Avenue, Bldg. 362
Lemont, IL 60439-4854

www.anl.gov